UCRL-JC-120920
PREPRINT
CONF-950793--42

Specification of Optical Components Using the Power Spectral Density Function

J. K. Lawson, C. R. Wolfe, K. R. Manes,
J. B. Trenholme, D. M. Aikens, and R. E. English, Jr.

This paper was prepared for submittal to the
SPIE's 40th Annual Meeting
San Diego, CA
July 9-14, 1995

June 20, 1995

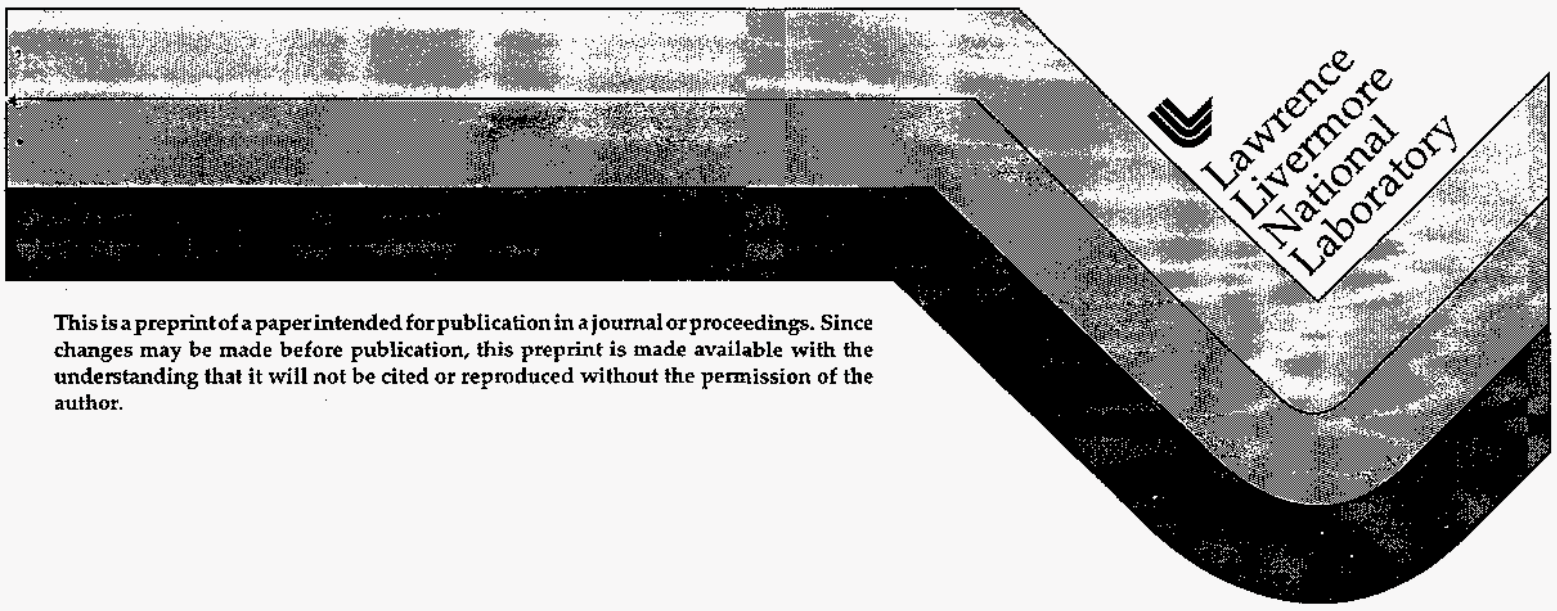

DISCLAIMER

Portions of this document may be illegible in electronic image products. Images are produced from the best available original document.

Specification of optical components using the power spectral density function

J.K. Lawson, C.R. Wolfe, K.R. Manes, J.B. Trenholme,
D.M. Aikens, R.E. English, Jr.

Lawrence Livermore National Laboratory
Livermore, CA 94551

ABSTRACT

This paper describes the use of Fourier techniques to characterize the wavefront of optical components, specifically, the use of the power spectral density, (PSD), function. The PSDs of several precision optical components will be shown. Many of the optical components of interest to us have square, rectangular or irregularly shaped apertures with major dimensions up-to 800 mm. The wavefronts of components with non-circular apertures cannot be analyzed with Zernicke polynomials since these functions are an orthogonal set for circular apertures only. Furthermore, Zernicke analysis is limited to treating low frequency wavefront aberrations; mid-spatial scale and high frequency error are expressed only as "residuals." A more complete and powerful representation of the optical wavefront can be obtained by Fourier analysis in 1 or 2 dimensions. The PSD is obtained from the amplitude of frequency components present in the Fourier spectrum. The PSD corresponds to the scattered intensity as a function of scattering angle in the wavefront and can be used to describe the intensity distribution at focus. The shape of a resultant wavefront or the focal spot of a complex multi-component laser system can be calculated and optimized using the PSDs of individual optical components which comprise it.

Keywords:
power spectral density, optical component specification, wavefront, Fourier analysis

1. INTRODUCTION

The Laser Program at Lawrence Livermore National Laboratory is investigating aspects of the design of high power solid-state laser systems, including the proposed Inertial Confinement Fusion (ICF) National Ignition Facility. In order to meet NIF performance and cost goals, the design of this laser system will push current laser technology to the limits of performance.[1] As such, the specification of the optics in the system plays a critical role in the design. In high power solid-state laser systems, phase modulations in the beam due to imperfections in the optics are transformed into intensity modulations. These intensity modulations can undergo non-linear gain when they occur at certain spatial frequencies.[2] Surface roughness of the optics also causes scatter and divergence in the laser beam. These are critical aspects of the system performance. Specification of the optics must include information about the spatial frequency of the phase errors present, in addition to more conventional information such as surface roughness and figure error.

Optical specifications have been experiencing a revolution over recent years, due partially to increased performance requirements and partially by increased measurement capability. X-ray optics and other applications requiring control of surface roughness have driven the development of analytic techniques specifying, in detail, aspects of-surface roughness and scattering behavior.[3-5] Standards now being proposed will not specify surface roughness in terms of a single number, but instead use the 2D PSD function.[6] These analytic techniques have a broad basis of applicability. Our study to optimize the performance versus cost of proposed solid-state laser systems has determined that specifications based on the PSD are the most effective for controlling mid-spatial wavelength errors. Such errors, commonly generated by cost effective, deterministic finishing techniques, can be damaging to the laser, as well as causing energy loss and inability to focus the energy on target. We have developed a Fourier technique using the PSD function to analyze high spatial resolution, phase-shifting interferometric data from prototypic optics. These tools have enabled us to quantify the spatial frequency content of the optical surfaces proposed for the NIF.

2. SPATIAL FREQUENCY REGIMES OF INTEREST

For our application, transmitted wavefront errors can be broken down into three spatial frequency regimes: long spatial period errors (figure), mid spatial period errors (ripple), and short spatial period errors (roughness). The long spatial frequency regimes includes any errors whose gradient results in energy still within the acceptance angle of the laser target. For NIF, this corresponds to errors with spatial periods longer than 33 mm and includes the classical Seidel third order aberrations such as coma and astigmatism, as well as other higher order functions. Sensitivity to these errors is low, and amplitudes as large as sixth wave peak-to-valley can be tolerated. As such, wavefront errors of this type can be controlled using conventional optics specifications such as RMS, Peak-to-Valley, and wavefront gradient specifications.

Short spatial period phase errors, i.e. errors smaller than 120 μm, in general, do not create high intensity modulation through non-linear processes in the solid-state laser system. Portions of the beam affected by these errors diffract quickly out of the main laser beam or are removed at the spatial filter pinhole. These errors are result in a surface and bulk scattering loss and can be adequately controlled through a conventional RMS or scattering specification.

We define a mid spatial wavelength regime as any phase error whose gradient results in light scattered into angles which are not accepted by the target, but are subject to non-linear growth. For the NIF, this includes any modulation from 33 mm to .120 mm in spatial period. Errors in this mid spatial wavelength regime pose a serious threat to the high-power laser as a source of damaging intensity and are becoming increasingly common as cost considerations drive the industry toward highly deterministic finishing processes. Errors of this type are difficult to control using an RMS or Peak-to-Valley specification, since the non-linear gain which can be experienced by these errors varies by orders of magnitude depending on the spatial frequency. Our goal is to develop

specifications based on the PSD that can be derived from modeling of the laser propagation, which do not overly constrain the manufacturing process used to fabricate the materials and surfaces.

3. APPROACH

With the advent of phase-shifting interferometry and high resolution solid-state cameras, the spatial resolution and information content of phase measurements has grown markedly over that available from static fringe analysis. We benefit from this growth by utilizing the new measurement techniques. The wavefront measurements reported here have been obtained using several phase-shifting interferometers available at Lawrence Livermore National Lab.[7] These instruments provide two dimensional arrays of wavefront information, typically expressed as waves at HeNe (6328 Å), over apertures from approximately 200 microns square to 300 mm square. We use Fourier techniques to analyze wavefront data. There exist in the literature several treatments of Fourier analysis and the power spectral density function for this type of application.[4,8] However, to insure clarity in the following presentation, we will summarize the process by which we go from an optical measurement to the analysis of the PSD.

3.1 Fourier domain

For our purposes, we want to express the measurement of the phase retardation of a transmissive optic (or, alternately, the phase retardation due to the reflection of a reflective optics) in terms of its spatial frequencies. In one dimension, we can write[9] the phase, $\phi(x)$, as a function of spatial frequency, ν, i.e.

$$\Phi(\nu) = \int_{-\infty}^{\infty} \phi(x)\, e^{-j2\pi\nu x}\, dx. \qquad (1)$$

In two dimensions, we express the phase, $\phi(x,y)$, as

$$\Phi(\nu_x,\nu_y) = \iint_{-\infty}^{\infty} \phi(x,y)\, e^{-j2\pi(\nu_x x+\nu_y y)}\, dx\, dy. \qquad (2)$$

For a transmissive optic, $\phi(x)$ or $\phi(x,y)$ corresponds to the optical path difference through the component, whereas for a reflective optic at normal incidence, the functions correspond to twice the magnitude of the surface contour. In reality, we deal with a continuous function of finite length and finite spatial frequency content. Specifically, we measure a set of N discrete, evenly spaced data points, $\phi(n)$, along a length, ℓ, or a similar array of N_x by N_y measurements, $\phi(m,n)$, over an area, ℓ_x by ℓ_y. The frequency content of the finite scan length is limited to discrete frequencies less that the Nyquist cutoff frequency. Thus, we calculate using standard computational packages the finite Fourier Transform,[10]

$$\Phi(\nu) = 1/N \sum_{n=0}^{N-1} \phi(n)\, e^{-j2\pi\nu x/N} \tag{3}$$

and

$$\Phi(\nu_x,\nu_y) = 1/(Nx \bullet Ny) \sum_{m=0}^{Nx-1} \sum_{n=0}^{Ny-1} \phi(m,n)\, e^{-j2\pi(\nu_x x/ N_x + \nu_y y/N_y)}. \tag{4}$$

The effect of the finite sample is mitigated by the use of a windowing function. Specifically, we use a Hanning window in both the 1D and 2D analysis. This broadens (or 'blurs') the resulting width of the spatial frequency structure, but eliminates frequencies generated by the discontinuities at the edge of the sample. We also correct for the loss of signal due to the application of the windowing function, ensuring that subsequent calculations of the PSD retain information on the surface roughness.[11]

We can calculate the value of the spatial frequencies as

$$\nu\,(n) = n / \ell \qquad \text{where } -(N/2 -1) < n < N/2 +1 \tag{5}$$

and, in the 2D case,

$$\nu_x\,(m) = m / \ell_x \qquad \text{where } -(N_x/2 -1) < m < N_x/2 +1 \tag{6a}$$

$$\nu_y\,(n) = n / \ell_y. \qquad -(N_y/2 -1) < n < N_y/2 +1 \tag{6b}$$

Variations in optical thickness of a transmissive optic or the roughness of the reflective surface can be calculated from the root mean square of the function,

$$rms_{1D} = \sqrt{\left(\sum_{n=0}^{N-1} \phi^2(i) / N\right)} \tag{7}$$

or in two dimensions,

$$rms_{2D} = \sqrt{\left(\sum_{m=0}^{Nx-1} \sum_{n=0}^{Ny-1} \phi^2(i,j) /(N_x \bullet N_y)\right)}. \tag{8}$$

When the Fourier pair being evaluated correspond to distance and spatial frequency, Parseval's theorem becomes a statement of rms distance.[12] That is,

$$rms_{1D} = \sqrt{\left(\sum_{n=0}^{N-1} | \Phi(\nu) |^2\right)} \tag{9}$$

and

$$rms_{2D} = \sqrt{\left(\sum_{m=0}^{Nx-1} \sum_{n=0}^{Ny-1} | \Phi(\nu_x,\nu_y) |^2\right)}. \tag{10}$$

3.2 PSD

We calculate the PSD using the formula

$$PSD(\nu) = \Phi^*(\nu) \bullet \Phi(\nu) \bullet \ell \tag{11}$$

or in the 2D case,

$$PSD(\nu_x,\nu_y) = \Phi^*(\nu_x,\nu_y) \bullet \Phi(\nu_x,\nu_y) \bullet \ell_x \bullet \ell_y . \tag{12}$$

While the PSD has the advantage of being a real quantity which expresses the spectral distribution of the surface roughness, it does not possess any relative phase information. Thus, specifications based on the PSD do not uniquely specify a given wavefront, but instead a family of wavefronts, each possessing similar spatial frequencies without necessarily being correlated with one another. Since the PSD in our case is the spectral distribution of the surface roughness, we can calculate the rms surface roughness of any spatial frequency band (ν_1 - ν_2) by integrating the PSD over that band. That is,

$$rms_{1D}(\nu_1 - \nu_2) = \sqrt{\left(\sum_{\nu=\nu_1}^{\nu_2} PSD(\nu) \bullet \Delta\nu\right)} \tag{13}$$

where $\Delta\nu = (\ell)^{-1}$ and, equivalently, for a 2D frequency range (ν_{x1} - ν_{x2}, ν_{y1} - ν_{y2})

$$rms_{2D}(\nu_{x1} - \nu_{x2}, \nu_{y1} - \nu_{y2}) = \sqrt{\left(\sum_{\nu_x=\nu_{x1}}^{\nu_{x2}} \sum_{\nu_y=\nu_{y1}}^{\nu_{y2}} PSD(\nu_x,\nu_y) \bullet \Delta\nu_x \bullet \Delta\nu_y\right)} \tag{14}$$

where $\Delta\nu_x = (\ell_x)^{-1}$ and $\Delta\nu_y = (\ell_y)^{-1}$. By inspection, Eq. 13 and 14 are equivalent to Eq. 9 and 10.

3.3 1D vs 2D

Although the actual calculations are similar in 1D and 2D, certain aspects of the two analyses strongly differ. A 1D profile across a surface samples only a small portion of the surface and is limited by low signal to noise. 2D calculations improve the signal to noise greatly by using all available data to build the Fourier spectrum. The 1D results can be improved by taking multiple profiles and averaging the resulting PSDs. In the 1D calculations presented below, we are taking ten profiles across the surface, all taken in the same orientation. Alternately, we can compute a 1D PSD by integrating over one of the two variables in the 2D PSD, i.e.,

$$PSD(\nu_x) = \int_{-\infty}^{\infty} PSD(\nu_x,\nu_y)\ dy \tag{15}$$

or alternately for discrete sums,

$$PSD(\nu_x) = \sum_{\nu_y=\nu_{y1}}^{\nu_{y2}} PSD(\nu_x,\nu_y)\ \Delta y. \tag{16}$$

This approach only makes sense if the direction over which the integration is done is perpendicular to the direction of peak modulation. We accomplish this by calculating the 2D PSD, determining the orientation of the peak values, and integrating along the perpendicular direction. This result can then be compared with the results of the 1D analysis when the 1D profiles are taken along the direction of peak modulation.

While 1D analysis is conceptually easier to understand, actual wavefronts are often not uniformly random or modulated only along one direction, i.e. cases which can easily characterized by a 1D description. Some of the wavefronts of optics which we are measuring have highly complex structure. Specifications are best made based on a 2D analysis for these types of optics. Alternately, 1D specifications must be based upon the direction suffering the worst modulation. One of the primary drawbacks to making 2D specifications appears to be the limitations imposed by existing commercial software packages for the commonly used interferometers. Until 2D calculations become more prevalent, 2D specifications will require post-processing of the measured data using custom software similar to that which we have written.

3.4 PSD analysis program

The analytic approach outlined above has been incorporated into a computer program written in Interactive Data Language® (IDL). This language is a powerful graphics-oriented language developed by Research Systems, Inc. which makes array calculations easy to program. Standard image processing tools, such as FFT's and Hanning windows, are integral to the language. This allows us to write the necessary calculations in only a few lines of code. The 1D analysis program has been written separately from the 2D program, although the two may be merged at a later date.

4. RESULTS

We show sample results from these calculations in Figures 1-4. Figures 1 and 2 are the results of an analysis of a 38 mm x 38 mm scan of a piece of laser glass. Weak periodic modulations in the phasefront are observable in the scan. These modulations have a Peak-to -Valley of about 100 angstroms and result in an rms surface roughness of 17 angstroms, calculated over the aperture shown. Figure 1c demonstrates the variation in PSD calculated from 10 profiles (Fig. 1b) chosen approximately in the direction of peak modulation. The average of the 10 PSD's results in a peak value of approximately 3×10^6 angstrom^2 - micron. (Note: units listed here are those used during development of the software package. To scale from angstroms^2 - microns to nanometers^2 - millimeters, multiply the PSD shown by a factor of 10^{-5}.)

By comparison, the 2D analysis of the same data shows the PSD (Fig. 2b) is maximum at approximately 0.15 mm^{-1} with a peak value of 2×10^{16} angstrom^2 - micron^2 and a width of about 0.1 mm^{-1}. Integration of the 2D PSD over the direction orthogonal to the peak modulation results in the 1D PSD shown in Fig. 2d. The shape and magnitude of the 1D PSD derived from integrating the 2D PSD is very similar to that obtained from the

multiple 1D profiles. Notice also that the signal-to-noise is much improved in Fig. 2d from that in Fig. 1d.

Examining Fig. 2b and c in more detail, a second source of modulation is observed, aligned with the x-axis. A logarithmic plot of the PSD (Fig. 2c) show the wealth of detail present in the two dimensions. Accurate modeling of this type of phasefront cannot be done with a 1D description.

Figures 3 and 4 duplicate the figures discussed above, except that they deal with a 38 mm x 38 mm transmitted wavefront from a potassium di-hydrogen phosphate (KDP) crystal. The crystal had been finished using a diamond turning process and has an rms surface roughness of 58 angstroms over the wavefront shown. The 1D analysis shows a very strong peak (about 8×10^8 angstroms^2 - microns) at a spatial frequency of 0.075 mm^{-1} and a second peak (about 10^6 angstroms^2 - microns) at 0.7 mm^{-1}. These phase modulations are attributed to surface modulations induced by the diamond-turning process. The 2D analysis shows this structure as well as identifying another modulation along a different axis with a spatial frequency of about 0.8 mm^{-1}. This second modulation at a comparable frequency probably corresponds to the turning marks on the second surface. Again, the improvement in signal-to-noise is apparent by comparing Fig. 4d to Fig. 3d.

5. FUTURE DIRECTIONS

The results discussed above all show the same non-exponential downward trend in PSD with increase in frequency. In fact, the PSD of a given optic at a particular frequency calculated for two measurements at different magnifications do not give the same magnitude. This behavior is typical of data which do not adequately account for the frequency response of the instrument making the measurement.[13,14] Currently, we are measuring the optical transfer function (OTF) of the instruments which we are using. Analytically, we know that the OTF will primarily contain contributions from the interferometer optical system and from the detector. The complex optical system of the interferometers, however, makes calculation of the actual optical contribution problematic. Thus, we have chosen to determine the OTF experimentally. To do this, we measure a test pattern of known amplitude and spatial frequency content (an abrupt discontinuity of known height and known transition distance works well[15]). We then compare the Fourier amplitude calculated from the measurement to the Fourier amplitude known from calibration of the test pattern. The OTF(v) is the ratio of these two, i.e.

$$OTF(\nu) = \Phi(\nu)_{measurement} / \Phi(\nu)_{known}. \qquad (17)$$

Previous investigations have shown that deconvolution of the OTF from the data is effective and can be used to join measurements made over different apertures into one extended profile[3].

6. ACKNOWLEDGMENTS

This work has been conducted in support of the laser modeling and the optical specifications efforts for the National Ignition Facility at the Lawrence Livermore National Laboratory. The authors wish to thank L.J. Atherton, J. M. Auerbach, A. Demeris, J.T. Hunt, M. Kellam, and R.T. Maney for their assistance in measurements and/or their insight concerning this work. This work was performed under auspices of the U. S. Department of Energy by the Lawrence Livermore National Laboratory under contract No. W-7405-ENG-48.

7. REFERENCES

1. National Ignition Facility Conceptual Design Report, UCRL # PROP117093, August 1994.

2. For a description of the actual non-linear phenomena, see V.I. Bespalov and V.I. Talanov, "Filamentary structure of light beams in nonlinear liquids," JETP Lett. 3, pp. 307-310 (1966). For the application to solid-state lasers, see J.B. Trenholme, "1975 Laser Annual Report," Lawrence Livermore National Laboratory, UCRL-50021-75, pp. 237-241 (1975)) or J.T. Hunt and D.R. Speck, "Present and Future Performance of the Nova Laser System," Opt. Eng., v 28(4), p.464 (1989).

3. E.L. Church, T.V. Vorburger and J.C. Wyant, "Direct comparison of mechanical and optical measurements of the finish of precision machined optical surfaces", Optical Eng., v. 24, no. 3, pp. 388 - 395, (1985)

4. J.M. Bennett and L. Mattsson, *Introduction to Surface Roughness and Scattering* (Optical Society of America, Washington, D. C., 1989), pp. 28-29,44-50.

5. E.L. Church and P.Z. Takacs, "Specification of glacing and normal-incidence x-ray mirrors", Optical Eng., v. 34, no. 2, p. 353-360, (1995).

6. "Optics and optical instruments - indications in optical drawings," in *Draft International Standard ISO 10110 Part 8: Surface Texture*, (International Organization for Standardization, ISO/TC 172/SC 1/WG 2, Geneva, Switzerland).

7. C.R. Wolfe and J.K. Lawson, "The measurement and analysis of wavefront structure form large aperture ICF optics," Proceedings of the 1st Annual Solid State Lasers for Application to Inertial Confinement Fusion Conference, May 31- June 2, 1995, Monterey, CA, to be published.

8. J.M. Elson and J.M. Bennett, "Calculation of the power spectral density from surface profile data", Applied Optics, v. 34, no. 1, pp. 201-208, (1995).

9. J.E. Goodman, *Statistcal Optics*, (Wiley-Interscience, New York, NY, 1985), p. 528.

10. *IDL® Reference Guide*, (Research Systems, Inc., Boulder, CO, 1993).

11. F.J. Harris,"On the Use of Windows for Harmonic Analysis with the Discrete Fourier Transform", Proc. of the IEEE, v. 66(1), pp. 51-83 (1978).

12. D. F. Elliott and K.R. Rao, *FAST TRANSFORMS: Algorithms, Analyses, Applications,* (Academic Press, Orlando, FL, 1982), p. 53.

13. E.L. Church and P.Z. Takacs, "Effects of the optical transfer function in surface profile measurements", in *Surface Characterization and Testing II,* Proc. SPIE, v. 1164, pp. 46-59 (1989).

14. E.L. Church and P.Z. Takacs, "Instrumental effects in surface finish measurement,' in *Surface Measurement and Characterization,* Proc. SPIE , v. 1009, pp. 46-55 (1989).

15. P.Z. Takacs and E.L. Church, "A Step-Height Standard for Surface Profiler Calibration," in *Quality and reliability for optical systems,* Proc. SPIE, v. 1993, pp. 65-74 (1993).

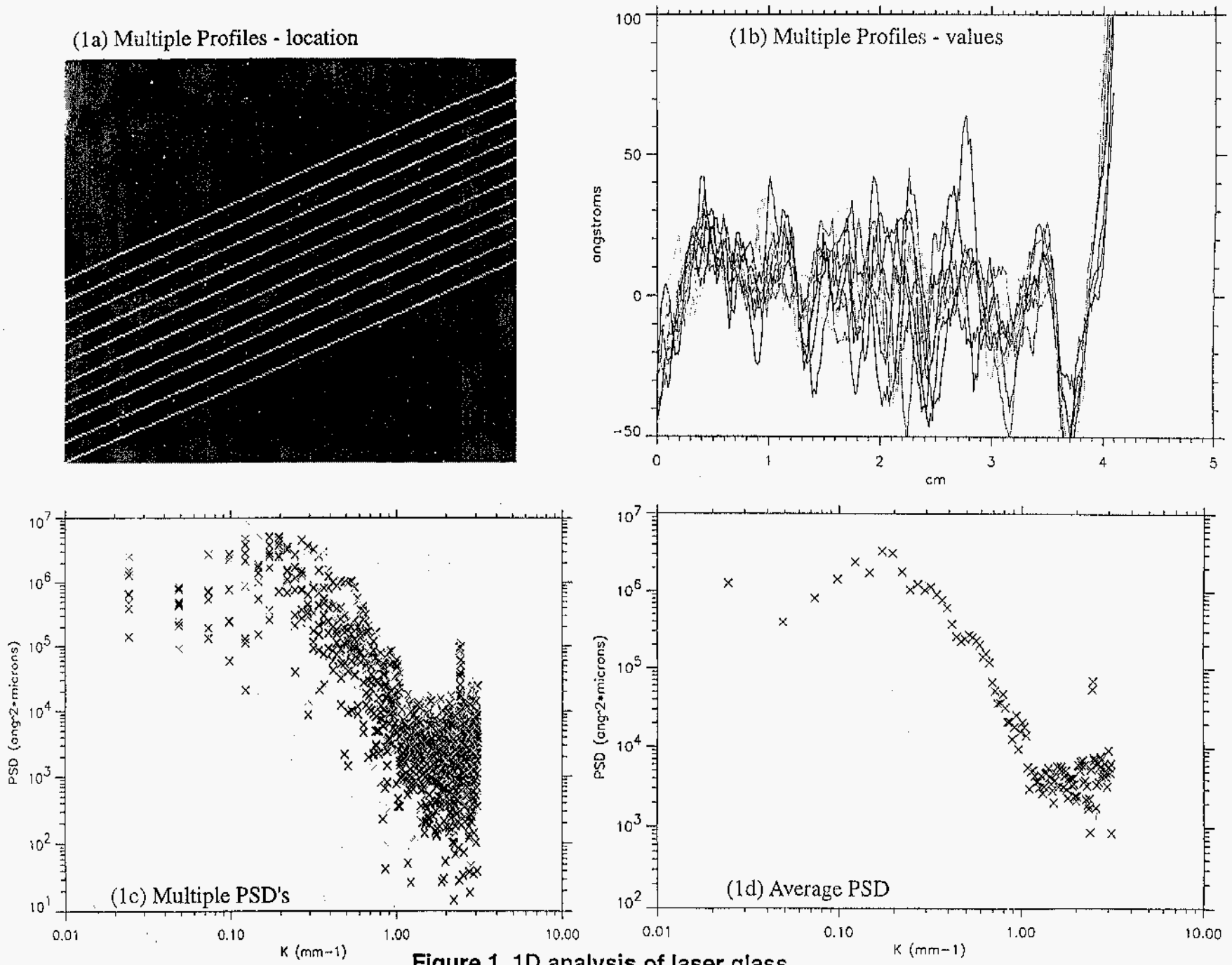

Figure 1. 1D analysis of laser glass

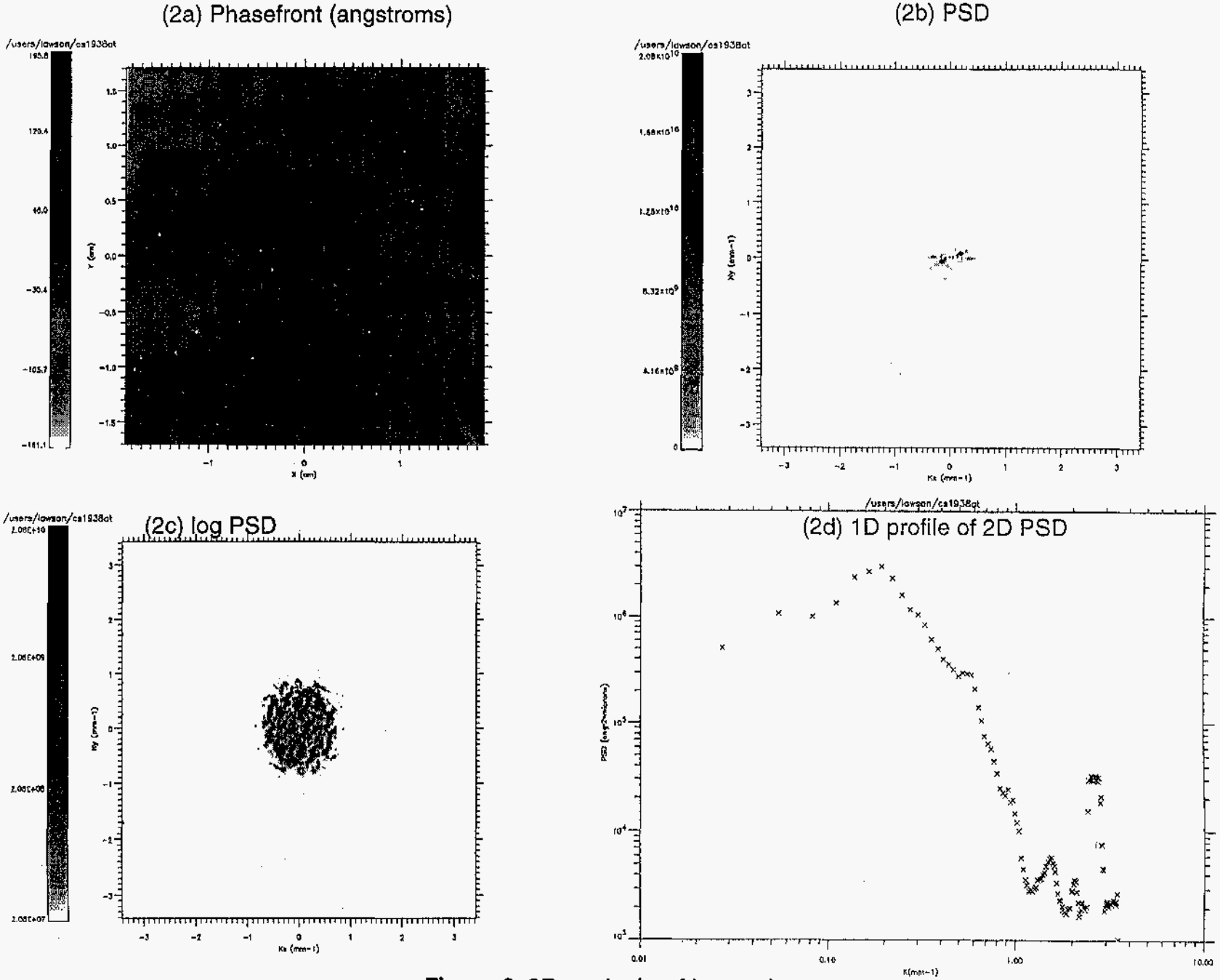

Figure 2. 2D analysis of laser glass

(3a) Multiple Profiles - location

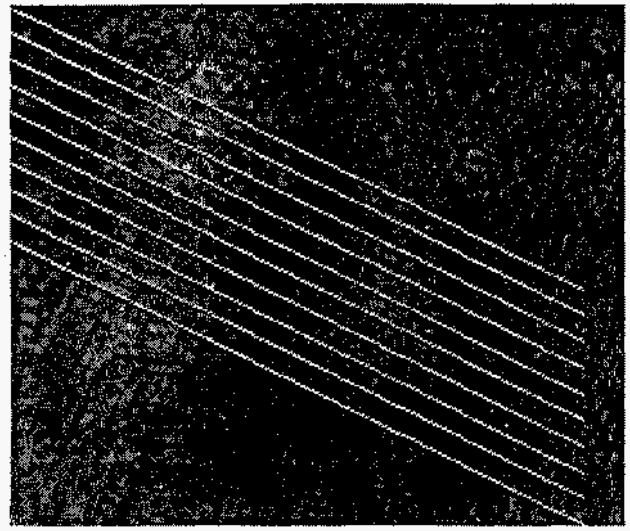

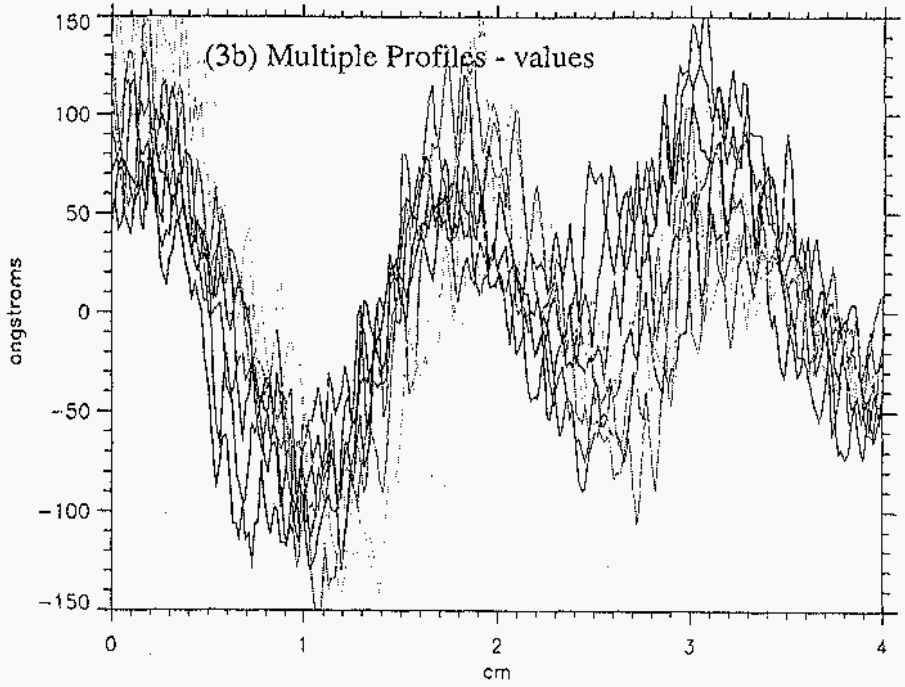

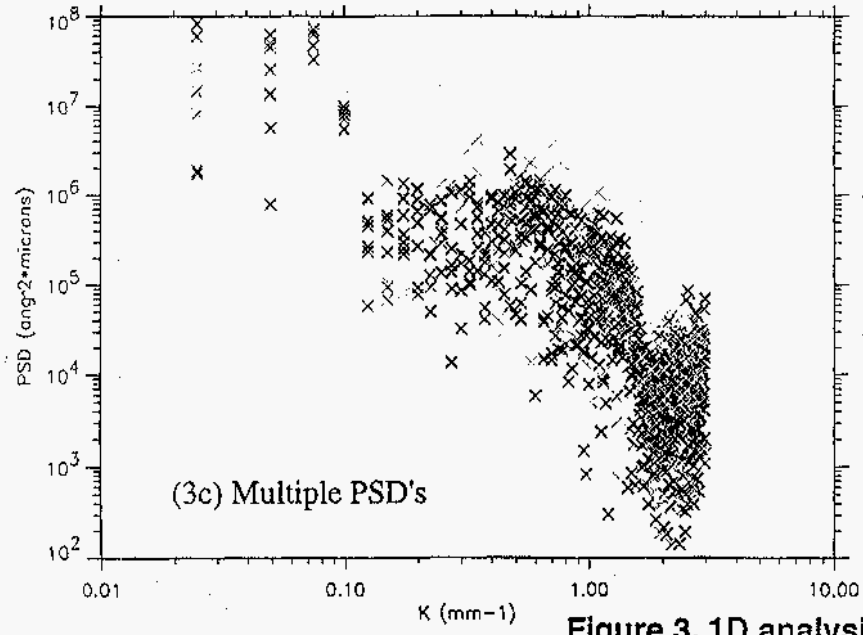

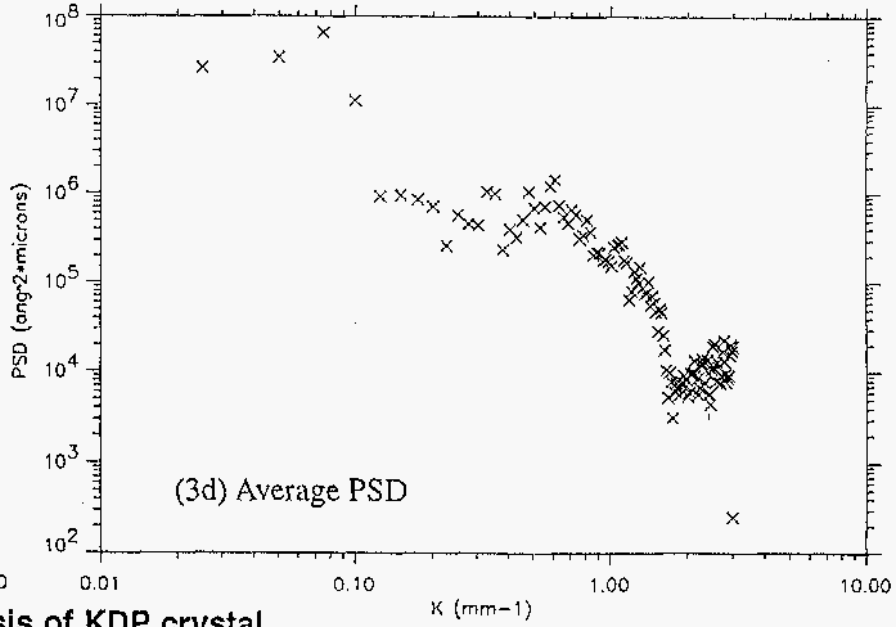

Figure 3. 1D analysis of KDP crystal

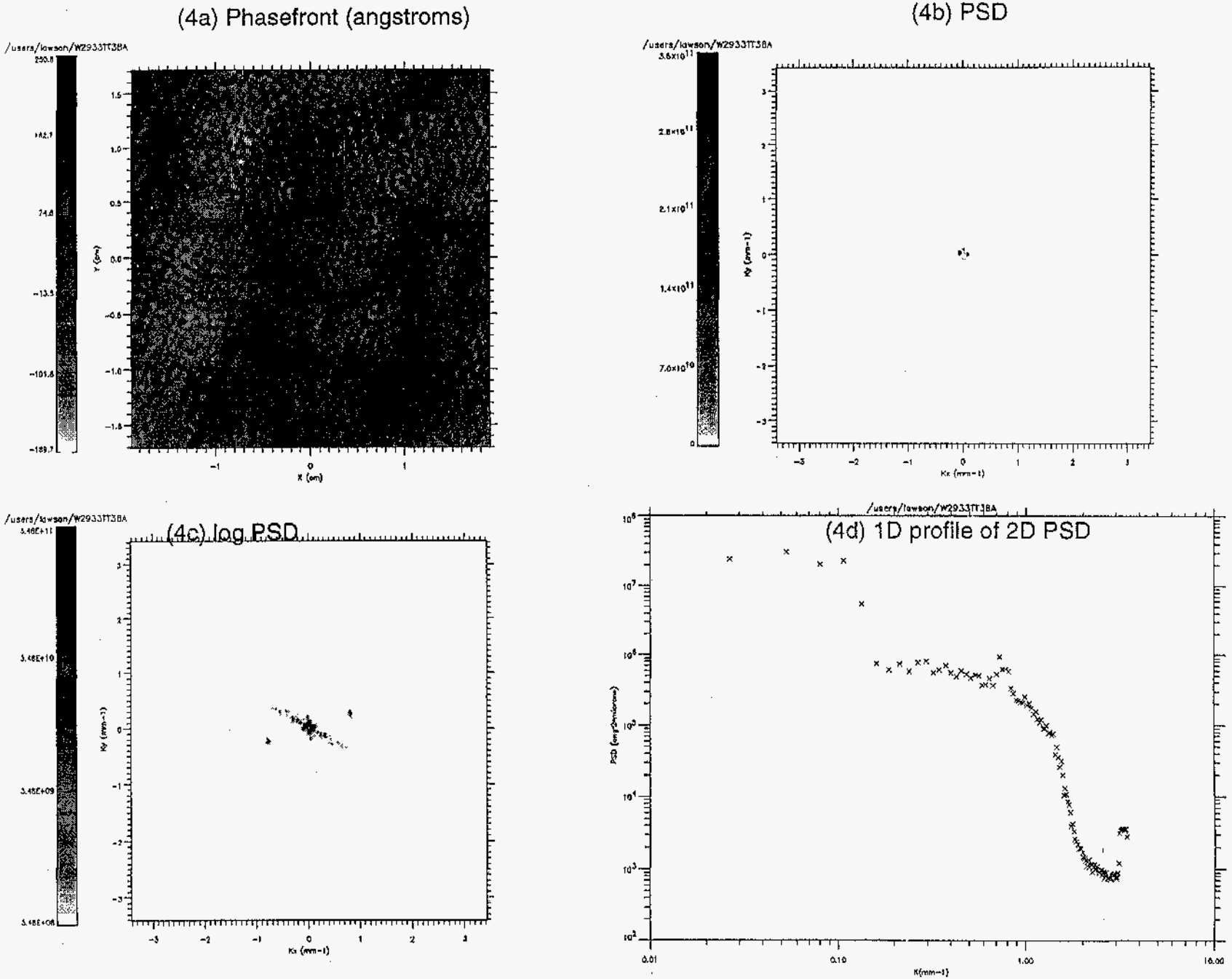

Figure 4. 2D analysis of KDP crystal